

# Measurement of the $\bar{B} \rightarrow D\ell\bar{\nu}$ Partial Width and Form Factor

## Parameters

(May 10, 2018)

### Abstract

We have studied the decay  $\bar{B} \rightarrow D\ell\bar{\nu}$ , where  $\ell = e$  or  $\mu$ . From a fit to the differential decay rate  $d\Gamma/dw$  we measure the rate normalization  $\mathcal{F}_D(1)|V_{cb}|$  and form factor slope  $\hat{\rho}_D^2$ , and, using measured values of  $\tau_B$ , find  $\Gamma(\bar{B} \rightarrow D\ell\bar{\nu}) = (12.0 \pm 0.9 \pm 2.1) \text{ ns}^{-1}$ . The resulting branching fractions are  $\mathcal{B}(\bar{B}^0 \rightarrow D^+\ell^-\bar{\nu}) = (1.87 \pm 0.15 \pm 0.32)\%$  and  $\mathcal{B}(B^- \rightarrow D^0\ell^-\bar{\nu}) = (1.94 \pm 0.15 \pm 0.34)\%$ . The form factor parameters are in agreement with those measured in  $\bar{B} \rightarrow D^*\ell\bar{\nu}$  decays, as predicted by heavy quark effective theory.

13.20.He,14.40.Nd,12.15.Hh,12.39Hg

M. Athanas,<sup>1</sup> P. Avery,<sup>1</sup> C. D. Jones,<sup>1</sup> M. Lohner,<sup>1</sup> C. Prescott,<sup>1</sup> J. Yelton,<sup>1</sup> J. Zheng,<sup>1</sup>  
 G. Brandenburg,<sup>2</sup> R. A. Briere,<sup>2</sup> A. Ershov,<sup>2</sup> Y. S. Gao,<sup>2</sup> D. Y.-J. Kim,<sup>2</sup> R. Wilson,<sup>2</sup>  
 H. Yamamoto,<sup>2</sup> T. E. Browder,<sup>3</sup> F. Li,<sup>3</sup> Y. Li,<sup>3</sup> J. L. Rodriguez,<sup>3</sup> T. Bergfeld,<sup>4</sup>  
 B. I. Eisenstein,<sup>4</sup> J. Ernst,<sup>4</sup> G. E. Gladding,<sup>4</sup> G. D. Gollin,<sup>4</sup> R. M. Hans,<sup>4</sup> E. Johnson,<sup>4</sup>  
 I. Karliner,<sup>4</sup> M. A. Marsh,<sup>4</sup> M. Palmer,<sup>4</sup> M. Selen,<sup>4</sup> J. J. Thaler,<sup>4</sup> K. W. Edwards,<sup>5</sup>  
 A. Bellerive,<sup>6</sup> R. Janicek,<sup>6</sup> D. B. MacFarlane,<sup>6</sup> P. M. Patel,<sup>6</sup> A. J. Sadoff,<sup>7</sup> R. Ammar,<sup>8</sup>  
 P. Baringer,<sup>8</sup> A. Bean,<sup>8</sup> D. Besson,<sup>8</sup> D. Coppage,<sup>8</sup> C. Darling,<sup>8</sup> R. Davis,<sup>8</sup> N. Hancock,<sup>8</sup>  
 S. Kotov,<sup>8</sup> I. Kravchenko,<sup>8</sup> N. Kwak,<sup>8</sup> S. Anderson,<sup>9</sup> Y. Kubota,<sup>9</sup> S. J. Lee,<sup>9</sup> J. J. O'Neill,<sup>9</sup>  
 S. Patton,<sup>9</sup> R. Poling,<sup>9</sup> T. Riehle,<sup>9</sup> V. Savinov,<sup>9</sup> A. Smith,<sup>9</sup> M. S. Alam,<sup>10</sup> S. B. Athar,<sup>10</sup>  
 Z. Ling,<sup>10</sup> A. H. Mahmood,<sup>10</sup> H. Severini,<sup>10</sup> S. Timm,<sup>10</sup> F. Wappler,<sup>10</sup> A. Anastassov,<sup>11</sup>  
 S. Blinov,<sup>11,1</sup> J. E. Duboscq,<sup>11</sup> D. Fujino,<sup>11,2</sup> K. K. Gan,<sup>11</sup> T. Hart,<sup>11</sup> K. Honscheid,<sup>11</sup>  
 H. Kagan,<sup>11</sup> R. Kass,<sup>11</sup> J. Lee,<sup>11</sup> M. B. Spencer,<sup>11</sup> M. Sung,<sup>11</sup> A. Undrus,<sup>11,1</sup> R. Wanke,<sup>11</sup>  
 A. Wolf,<sup>11</sup> M. M. Zoeller,<sup>11</sup> B. Nemati,<sup>12</sup> S. J. Richichi,<sup>12</sup> W. R. Ross,<sup>12</sup> P. Skubic,<sup>12</sup>  
 M. Bishai,<sup>13</sup> J. Fast,<sup>13</sup> E. Gerndt,<sup>13</sup> J. W. Hinson,<sup>13</sup> N. Menon,<sup>13</sup> D. H. Miller,<sup>13</sup>  
 E. I. Shibata,<sup>13</sup> I. P. J. Shipsey,<sup>13</sup> M. Yurko,<sup>13</sup> L. Gibbons,<sup>14</sup> S. Glenn,<sup>14</sup> S. D. Johnson,<sup>14</sup>  
 Y. Kwon,<sup>14</sup> S. Roberts,<sup>14</sup> E. H. Thorndike,<sup>14</sup> C. P. Jessop,<sup>15</sup> K. Lingel,<sup>15</sup> H. Marsiske,<sup>15</sup>  
 M. L. Perl,<sup>15</sup> D. Ugolini,<sup>15</sup> R. Wang,<sup>15</sup> X. Zhou,<sup>15</sup> T. E. Coan,<sup>16</sup> V. Fadeyev,<sup>16</sup>  
 I. Korolkov,<sup>16</sup> Y. Maravin,<sup>16</sup> I. Narsky,<sup>16</sup> V. Shelkov,<sup>16</sup> J. Staeck,<sup>16</sup> R. Stroynowski,<sup>16</sup>  
 I. Volobouev,<sup>16</sup> J. Ye,<sup>16</sup> M. Artuso,<sup>17</sup> A. Efimov,<sup>17</sup> M. Gao,<sup>17</sup> M. Goldberg,<sup>17</sup> D. He,<sup>17</sup>  
 S. Kopp,<sup>17</sup> G. C. Moneti,<sup>17</sup> R. Mountain,<sup>17</sup> S. Schuh,<sup>17</sup> T. Skwarnicki,<sup>17</sup> S. Stone,<sup>17</sup>  
 G. Viehhauser,<sup>17</sup> X. Xing,<sup>17</sup> J. Bartelt,<sup>18</sup> S. E. Csorna,<sup>18</sup> V. Jain,<sup>18</sup> K. W. McLean,<sup>18</sup>  
 S. Marka,<sup>18</sup> R. Godang,<sup>19</sup> K. Kinoshita,<sup>19</sup> I. C. Lai,<sup>19</sup> P. Pomianowski,<sup>19</sup> S. Schrenk,<sup>19</sup>  
 G. Bonvicini,<sup>20</sup> D. Cinabro,<sup>20</sup> R. Greene,<sup>20</sup> L. P. Perera,<sup>20</sup> G. J. Zhou,<sup>20</sup> B. Barish,<sup>21</sup>  
 M. Chadha,<sup>21</sup> S. Chan,<sup>21</sup> G. Eigen,<sup>21</sup> J. S. Miller,<sup>21</sup> C. O'Grady,<sup>21</sup> M. Schmidtler,<sup>21</sup>  
 J. Urheim,<sup>21</sup> A. J. Weinstein,<sup>21</sup> F. Würthwein,<sup>21</sup> D. W. Bliss,<sup>22</sup> G. Masek,<sup>22</sup> H. P. Paar,<sup>22</sup>  
 S. Prell,<sup>22</sup> V. Sharma,<sup>22</sup> D. M. Asner,<sup>23</sup> J. Gronberg,<sup>23</sup> T. S. Hill,<sup>23</sup> R. Kutschke,<sup>23</sup>  
 D. J. Lange,<sup>23</sup> S. Menary,<sup>23</sup> R. J. Morrison,<sup>23</sup> H. N. Nelson,<sup>23</sup> T. K. Nelson,<sup>23</sup> C. Qiao,<sup>23</sup>  
 J. D. Richman,<sup>23</sup> D. Roberts,<sup>23</sup> A. Ryd,<sup>23</sup> M. S. Witherell,<sup>23</sup> R. Balest,<sup>24</sup> B. H. Behrens,<sup>24</sup>  
 W. T. Ford,<sup>24</sup> H. Park,<sup>24</sup> J. Roy,<sup>24</sup> J. G. Smith,<sup>24</sup> J. P. Alexander,<sup>25</sup> C. Bebek,<sup>25</sup>  
 B. E. Berger,<sup>25</sup> K. Berkelman,<sup>25</sup> K. Bloom,<sup>25</sup> D. G. Cassel,<sup>25</sup> H. A. Cho,<sup>25</sup>  
 D. M. Coffman,<sup>25</sup> D. S. Crowcroft,<sup>25</sup> M. Dickson,<sup>25</sup> P. S. Drell,<sup>25</sup> K. M. Ecklund,<sup>25</sup>  
 R. Ehrlich,<sup>25</sup> A. D. Foland,<sup>25</sup> P. Gaidarev,<sup>25</sup> B. Gittelmann,<sup>25</sup> S. W. Gray,<sup>25</sup> D. L. Hartill,<sup>25</sup>  
 B. K. Heltsley,<sup>25</sup> P. I. Hopman,<sup>25</sup> J. Kandaswamy,<sup>25</sup> P. C. Kim,<sup>25</sup> D. L. Kreinick,<sup>25</sup>  
 T. Lee,<sup>25</sup> Y. Liu,<sup>25</sup> G. S. Ludwig,<sup>25</sup> J. Masui,<sup>25</sup> J. Mevissen,<sup>25</sup> N. B. Mistry,<sup>25</sup> C. R. Ng,<sup>25</sup>  
 E. Nordberg,<sup>25</sup> M. Ogg,<sup>25,3</sup> J. R. Patterson,<sup>25</sup> D. Peterson,<sup>25</sup> D. Riley,<sup>25</sup> A. Soffer,<sup>25</sup>  
 B. Valant-Spaight,<sup>25</sup> and C. Ward<sup>25</sup>

<sup>1</sup>University of Florida, Gainesville, Florida 32611

<sup>2</sup>Harvard University, Cambridge, Massachusetts 02138

---

<sup>1</sup>Permanent address: BINP, RU-630090 Novosibirsk, Russia.

<sup>2</sup>Permanent address: Lawrence Livermore National Laboratory, Livermore, CA 94551.

<sup>3</sup>Permanent address: University of Texas, Austin TX 78712

- <sup>3</sup>University of Hawaii at Manoa, Honolulu, Hawaii 96822
- <sup>4</sup>University of Illinois, Champaign-Urbana, Illinois 61801
- <sup>5</sup>Carleton University, Ottawa, Ontario, Canada K1S 5B6  
and the Institute of Particle Physics, Canada
- <sup>6</sup>McGill University, Montréal, Québec, Canada H3A 2T8  
and the Institute of Particle Physics, Canada
- <sup>7</sup>Ithaca College, Ithaca, New York 14850
- <sup>8</sup>University of Kansas, Lawrence, Kansas 66045
- <sup>9</sup>University of Minnesota, Minneapolis, Minnesota 55455
- <sup>10</sup>State University of New York at Albany, Albany, New York 12222
- <sup>11</sup>Ohio State University, Columbus, Ohio 43210
- <sup>12</sup>University of Oklahoma, Norman, Oklahoma 73019
- <sup>13</sup>Purdue University, West Lafayette, Indiana 47907
- <sup>14</sup>University of Rochester, Rochester, New York 14627
- <sup>15</sup>Stanford Linear Accelerator Center, Stanford University, Stanford, California 94309
- <sup>16</sup>Southern Methodist University, Dallas, Texas 75275
- <sup>17</sup>Syracuse University, Syracuse, New York 13244
- <sup>18</sup>Vanderbilt University, Nashville, Tennessee 37235
- <sup>19</sup>Virginia Polytechnic Institute and State University, Blacksburg, Virginia 24061
- <sup>20</sup>Wayne State University, Detroit, Michigan 48202
- <sup>21</sup>California Institute of Technology, Pasadena, California 91125
- <sup>22</sup>University of California, San Diego, La Jolla, California 92093
- <sup>23</sup>University of California, Santa Barbara, California 93106
- <sup>24</sup>University of Colorado, Boulder, Colorado 80309-0390
- <sup>25</sup>Cornell University, Ithaca, New York 14853

Exclusive semileptonic  $B$  meson decays provide information about both the weak and strong interactions of quarks. The rate for these decays is proportional to the square of the CKM matrix element  $|V_{cb}|$  [1], while the dynamics of these decays, as expressed in the decay form factors, provide information about the QCD potential which binds quarks together as hadrons [2,3]. Heavy quark effective theory (HQET) [4] has made it possible to extract values of  $|V_{cb}|$ , with relatively little model dependence, through a measurement of the decay rate at the point of zero recoil of the daughter meson. The decay  $\bar{B} \rightarrow D^* \ell \bar{\nu}$  has provided measurements of the decay rate at the point of zero recoil and the form factor slope, giving very accurate values of  $|V_{cb}|$  [5] and information about the shape of the Isgur-Wise function that describes the dynamics of heavy-to-heavy meson transitions.

The pseudoscalar-to-pseudoscalar decay  $\bar{B} \rightarrow D \ell \bar{\nu}$  can provide the same information, although it will be less precise because of the smaller overall decay rate for this mode than for  $\bar{B} \rightarrow D^* \ell \bar{\nu}$ , the smaller rate near the point of zero recoil, and  $\mathcal{O}(1/M_Q)$  corrections to the decay rate at that point that are not present in  $\bar{B} \rightarrow D^* \ell \bar{\nu}$ . However, this mode should yield a value of  $|V_{cb}|$  that is consistent with other measurements, and HQET predicts [6] that the form factor parameters should be very nearly the same as in the  $\bar{B} \rightarrow D^* \ell \bar{\nu}$  decay. In this Letter, we present a measurement of the differential decay rate  $d\Gamma/dw$  in the decay  $\bar{B} \rightarrow D \ell \bar{\nu}$ , from which we extract the decay rate normalization at the point of zero recoil and the form factor slope. The variable  $w = (M_B^2 + M_D^2 - q^2)/(2M_B M_D)$ , where  $q^2$  is the invariant mass squared of the lepton-neutrino system, is the kinematic variable of HQET, and is equal to the relativistic  $\gamma$  factor for the  $D$  meson in the  $B$  meson rest frame. From these results and the measured  $B$  lifetime, we obtain the partial width for the decay and convert it to branching fractions.

This study is based on an  $\Upsilon(4S)$  data sample of  $3.16 \text{ fb}^{-1}$  ( $3.34 \times 10^6$   $B\bar{B}$  pairs) accumulated by the CLEO experiment at the Cornell Electron Storage Ring (CESR). The CLEO detector [7] contains three concentric wire chambers that detect charged particles and a CsI(Tl) electromagnetic calorimeter that detects photons, all within a 1.5 T superconducting solenoid.

The undetected neutrino complicates analysis of semileptonic decays. Using the hermeticity of the CLEO detector, we reconstruct the neutrino by inferring its four-momentum from the missing energy ( $E_{\text{miss}} \equiv 2E_{\text{beam}} - \sum E_i$ ) and missing momentum ( $\vec{p}_{\text{miss}} \equiv -\sum \vec{p}_i$ ) in each event, where  $E_i$  and  $\vec{p}_i$  are the energy and momentum of each detected particle  $i$  in the event, as was done in the CLEO measurement of exclusive  $b \rightarrow u \ell \bar{\nu}$  decay rates [8]. In the process  $e^+e^- \rightarrow \Upsilon(4S) \rightarrow B\bar{B}$ , the total energy of the beams is imparted to the  $B\bar{B}$  system. At CESR, that system is at rest, so the neutrino combined with the signal lepton and  $D$  meson should satisfy the energy constraint  $\Delta E \equiv (E_{\bar{\nu}} + E_{\ell} + E_D) - E_{\text{beam}} = 0$  and the momentum constraint  $M_{\text{cand}} \equiv [E_{\text{beam}}^2 - |\vec{p}_{\bar{\nu}} + \vec{p}_{\ell} + \vec{p}_D|^2]^{\frac{1}{2}} = M_B$ . We select candidates with  $5.2650 \leq M_{\text{cand}} < 5.2875$  GeV and  $-100 \leq \Delta E < 500$  MeV; the requirement on  $\Delta E$  is asymmetric about zero to reject feeddown from  $\bar{B} \rightarrow D^* \ell \bar{\nu}$  decays, which have  $\Delta E$  values of about  $-150$  MeV when reconstructed as  $\bar{B} \rightarrow D \ell \bar{\nu}$  decays.

To suppress events in which  $\vec{p}_{\text{miss}}$  misrepresents  $\vec{p}_{\bar{\nu}}$ , we reject those events with multiple leptons or a total charge more than one unit from zero because they indicate other missing particles. We further require that  $M_{\text{miss}}^2 \equiv E_{\text{miss}}^2 - |\vec{p}_{\text{miss}}|^2$  for each event be consistent with zero. Surviving signal events show a resolution in  $|\vec{p}_{\text{miss}}|$  of 110 MeV/ $c$ . Because the resolution on  $E_{\text{miss}}$  is about 2.1 times larger, we take  $(E_{\bar{\nu}}, \vec{p}_{\bar{\nu}}) = (|\vec{p}_{\text{miss}}|, \vec{p}_{\text{miss}})$ .

Information from calorimeter and tracking measurements including specific ionization is combined to identify electrons with  $p > 600$  MeV/ $c$  over 90% of the solid angle. Particles are considered muons if they register hits in counters deeper than 5 interaction lengths over the polar angle range  $|\cos\theta| < 0.85$ . Candidate leptons must have  $0.8 \leq p_\ell < 2.4$  GeV/ $c$ , where the lepton identification efficiency averages more than 90%; the probability that a hadron is misidentified as an electron (muon), a “fake lepton”, is about 0.1% (1%).

The leptons and neutrinos are then combined with  $D$  mesons, which are identified in the decay modes  $D^0 \rightarrow K^-\pi^+$  and  $D^+ \rightarrow K^-\pi^+\pi^+$ . (The charge conjugate mode is always implied.) Hadron mass assignments are made by requiring that the kaon and lepton have the same charge. To reduce large backgrounds to  $D^+ \rightarrow K^-\pi^+\pi^+$  decays from random track combinations, we require that the  $D^+$  daughter pions (kaon) have measured specific ionization values consistent with the assumed particle hypothesis within 3.5 (3) standard deviations.  $D^0$  candidates are required to have invariant mass satisfying  $1.850 \leq M_{K\pi} < 1.880$  GeV, and  $D^+$  candidates to satisfy  $1.855 \leq M_{K\pi\pi} < 1.885$  GeV. This  $\pm 15$  MeV range is about twice the experimental resolution on the invariant mass. Since the  $D$  must come from a  $B$  decay, we require  $p_D < 2.6$  GeV/ $c$ . We also require that the angle between the directions of the  $D$  candidate and the lepton-neutrino system have a physical value; the angle is calculated from the  $D$  meson and lepton momenta and the beam energy only, without examining the missing momentum.

Backgrounds arise from  $e^+e^- \rightarrow q\bar{q}/\tau^+\tau^-$  (continuum), fake leptons, random track combinations that form  $D$  candidates, feeddown from other  $\bar{B} \rightarrow DX\ell\bar{\nu}$  decays, and random combinations of  $D$  candidates and leptons from different parent  $B$  mesons. The continuum backgrounds are reduced by requiring that the ratio of Fox-Wolfram moments  $H_2/H_0$  [9] be less than 0.4. Backgrounds from  $\bar{B} \rightarrow D^*X\ell\bar{\nu}$  decays are reduced by eliminating events that include  $D\pi$  or  $D\gamma$  pairs that are consistent with  $D^*$  decay. We find 303  $D^0\ell^-\bar{\nu}$  and 714  $D^+\ell^-\bar{\nu}$  candidates that satisfy all of these requirements. The average reconstruction efficiency, as determined by a Monte Carlo simulation of the CLEO detector, is 2.82% for  $B^- \rightarrow D^0\ell^-\bar{\nu}$  events and 2.57% for  $\bar{B}^0 \rightarrow D^+\ell^-\bar{\nu}$  events. Figure 1 shows the  $M_{\text{cand}}$  distribution observed in the data.

We estimate the continuum background using data collected 60 MeV below the  $\Upsilon(4S)$  energy and the fake lepton background by applying measured fake rates to nonleptonic data. We estimate backgrounds from random track combinations that form  $D$  candidates using events in sideband regions on either side of the  $K^-\pi^+(\pi^+)$  invariant mass signal region under the assumption that the magnitude of this background is linear in  $K^-\pi^+(\pi^+)$  invariant mass. This is the largest background in the  $D^+\ell^-\bar{\nu}$  sample.

Feeddown backgrounds are modeled through Monte Carlo simulations, using an event generator that accounts for all angular correlations among the decay products, and a full simulation of the CLEO detector. The magnitude of the  $\bar{B} \rightarrow D^*\ell\bar{\nu}$  background is normalized to the measured rate for this decay [10]. This is the largest background in the  $D^0\ell^-\bar{\nu}$  sample, as the kinematics of the signal and background decays are so similar, and because  $D^*$  mesons are more likely to decay to a  $D^0$  than to a  $D^+$ .  $\bar{B} \rightarrow D^{**}\ell\bar{\nu}$  processes, where  $D^{**}$  represents a variety of charm mesons with radial and angular excitations and nonresonant  $D^{(*)}\pi$  states, are modeled with the ISGW2 [2] and Goity and Roberts [11] models. We normalize these backgrounds to a set of rates [12] that are consistent with existing measurements [13] and the total  $B$  semileptonic decay rate and lepton momentum spectrum [14].

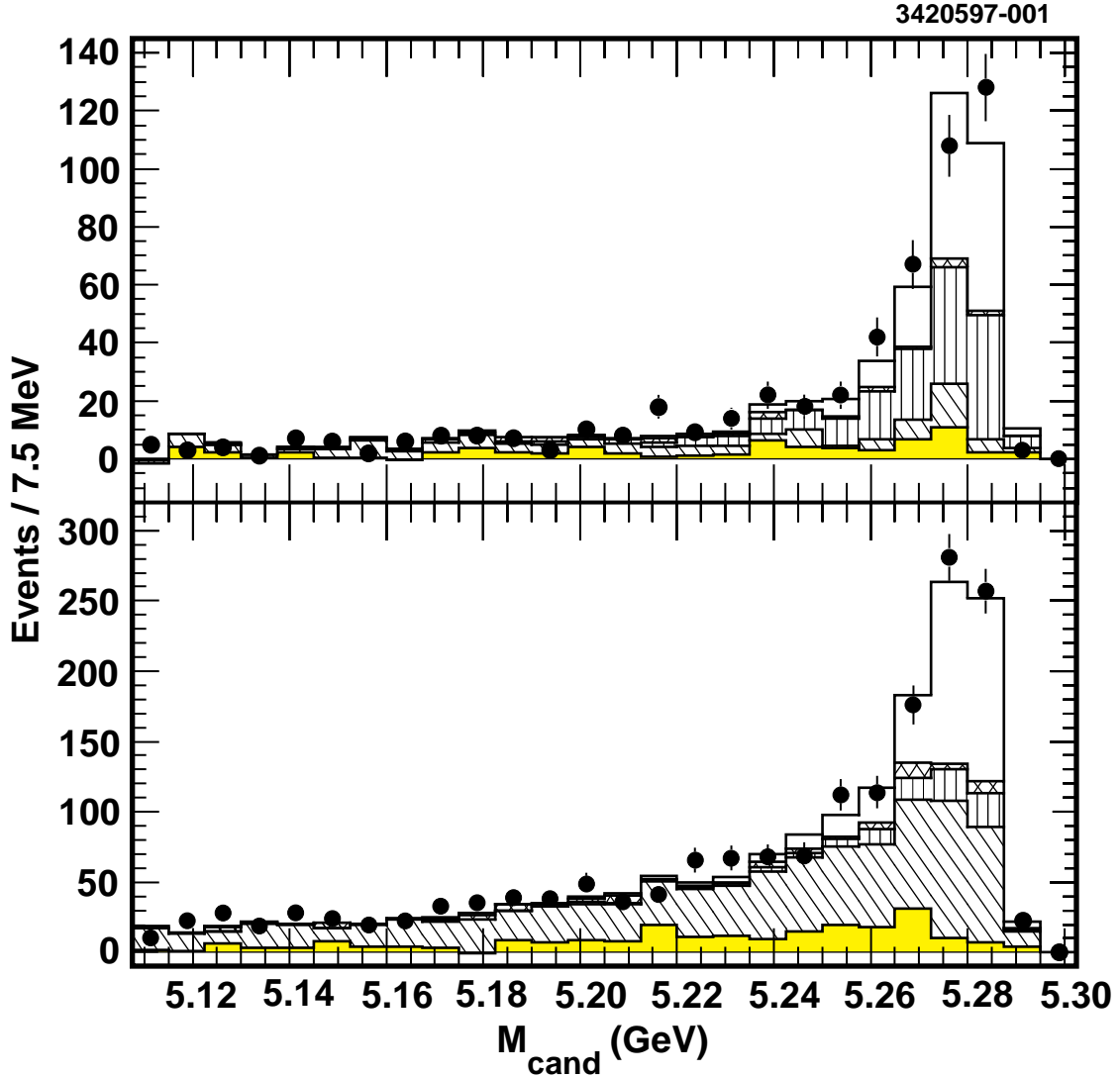


FIG. 1.  $M_{\text{cand}}$  distributions for the  $D^0 \ell^- \bar{\nu}$  (top) and  $D^+ \ell^- \bar{\nu}$  (bottom) modes. The points are the data, the shaded component is the continuum and fake lepton background, the diagonal hatch is the combinatoric background, the vertical hatch is the  $\bar{B} \rightarrow D^* \ell \bar{\nu}$  feeddown, and the crosshatch is the  $\bar{B} \rightarrow D^{**} \ell \bar{\nu}$  and other backgrounds. The unshaded area is the prediction of a Monte Carlo simulation of the signal, normalized to the measured decay rate.

TABLE I. Event yields and background estimates. Errors are statistical only.

	$D^0\ell^-\bar{\nu}$	$D^+\ell^-\bar{\nu}$
Total Yield	$303.0 \pm 17.4$	$714.0 \pm 26.7$
Continuum	$17.3 \pm 5.8$	$46.2 \pm 9.4$
Combinatoric	$26.1 \pm 4.6$	$256.5 \pm 10.8$
Fake lepton	2.9	2.3
$\bar{B} \rightarrow D^*\ell\bar{\nu}$	107.2	62.6
$\bar{B} \rightarrow D^{**}\ell\bar{\nu}$	5.3	9.9
Other	-0.1	13.6
Corrected Yield	$144.3 \pm 18.9$	$322.8 \pm 30.3$

Remaining backgrounds, such as those from random combinations of  $D$  mesons and leptons and those from misreconstructed  $D$  mesons not accounted for in the combinatoric background estimate, are modeled by a Monte Carlo simulation that reproduces the general features of  $B$ -meson decay, including the inclusive-lepton and  $D$  momentum distributions. The magnitudes of the various backgrounds are summarized in Table I. Figure 1 shows the  $M_{\text{cand}}$  distributions of the backgrounds. After accounting for these backgrounds in our sample, the lepton momentum and decay angle distributions for selected events are consistent with  $\bar{B} \rightarrow D\ell\bar{\nu}$  decays.

To extract the form factor parameters and partial width, we construct the distribution

$$\frac{d\Gamma}{dw} = \frac{1}{4N_{\Upsilon(4S)}} \left[ \frac{N_0(w)}{\tau_{B^-}\mathcal{B}_{D^0\epsilon_0}(w)} + \frac{N_+(w)}{\tau_{\bar{B}^0}\mathcal{B}_{D^+\epsilon_+}(w)} \right],$$

where  $N_{\Upsilon(4S)}$  is the number of  $\Upsilon(4S)$  events,  $\epsilon(w)$  is the reconstruction efficiency as a function of  $w$ ,  $\tau_B$  is the  $B$  lifetime, and  $\mathcal{B}$  is the appropriate  $D \rightarrow K^-\pi^+(\pi^+)$  branching fraction [10]. By combining the two decay modes in this fashion and assuming that the partial widths of the two modes are equal, the results are independent of the division of  $\Upsilon(4S)$  decays between  $B^+B^-$  and  $B^0\bar{B}^0$ . This distribution is shown in Figure 2a.

The  $d\Gamma/dw$  distribution for  $\bar{B} \rightarrow D\ell\bar{\nu}$  decays is [6]

$$\frac{d\Gamma}{dw} = \frac{G_F^2|V_{cb}|^2}{48\pi^3}(m_B + m_D)^2(m_D\sqrt{w^2 - 1})^3\mathcal{F}_D(w)^2.$$

The function  $\mathcal{F}_D(w)$  is the decay form factor, which can be parameterized by the expression

$$\mathcal{F}_D(w) = \mathcal{F}_D(1)(1 - \hat{\rho}_D^2(w - 1) + \hat{c}_D(w - 1)^2).$$

In the limit of infinitely heavy quarks,  $\mathcal{F}_D(w)$  becomes the Isgur-Wise function  $\xi(w)$ , and HQET predicts that  $\mathcal{F}_D(1) = 1$ ; for finite mass quarks,  $\mathcal{F}_D(1)$  can be estimated in the framework of HQET [4]. The values of  $\hat{\rho}_D^2$  and  $\hat{c}_D$  are unknown; many previous form factor measurements have set  $\hat{c}_D = 0$ . We follow this convention, but explore our sensitivity to this assumption using various models that provide relations between  $\hat{\rho}_D^2$  and  $\hat{c}_D$ . We perform a  $\chi^2$  fit of our  $d\Gamma/dw$  distribution to the convolution of the expected form with a function that accounts for detector resolution in  $w$  ( $\pm 0.015$ ). We allow two free parameters, the rate normalization  $\mathcal{F}_D(1)|V_{cb}|$  and the form factor slope  $\hat{\rho}_D^2$ . By integrating the fit over the

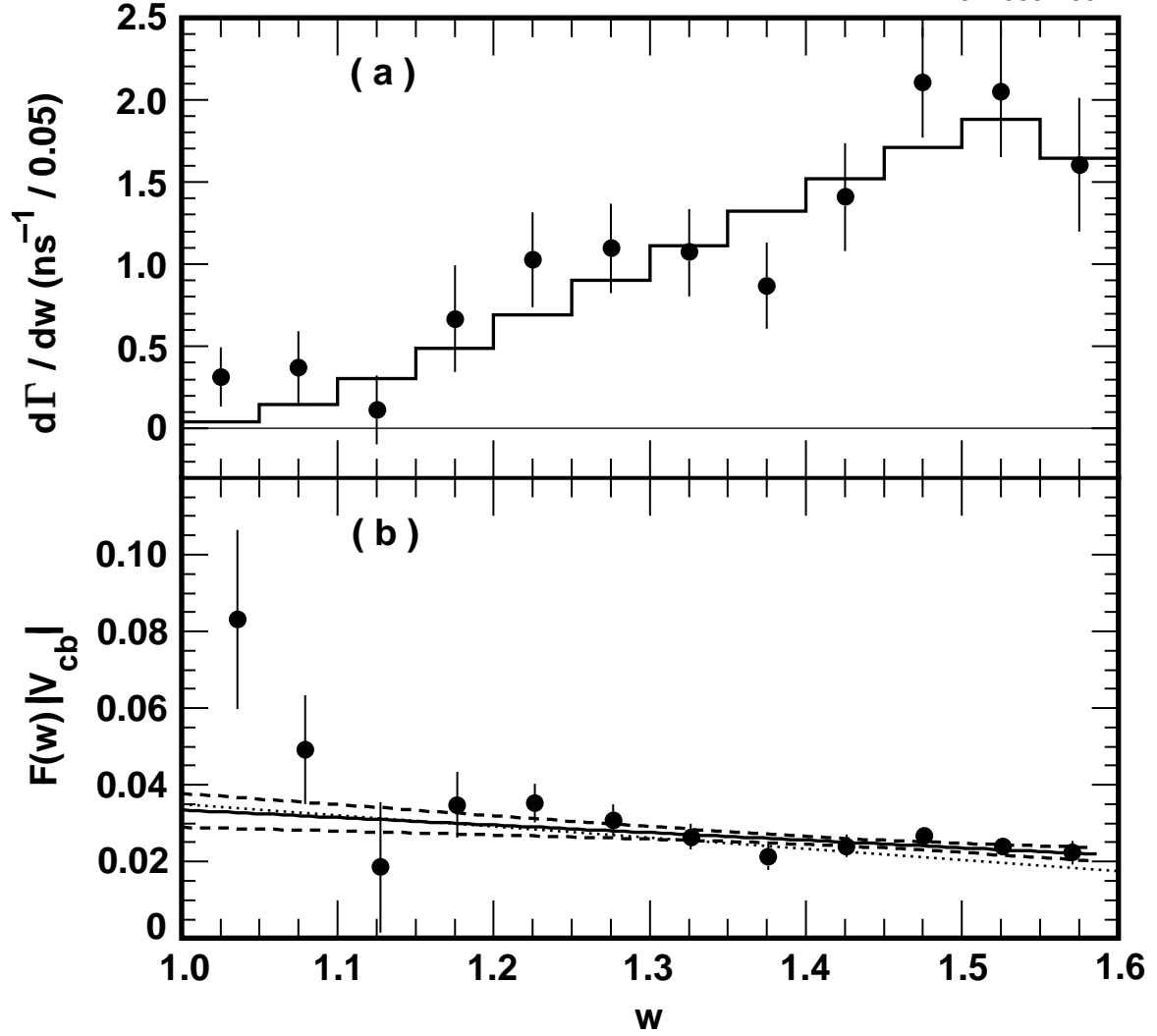


FIG. 2. (a)  $d\Gamma/dw$  distribution from the data (points), and the result of the  $c = 0$  fit to the distribution (histogram). (b) Measured values of  $\mathcal{F}_D(w)|V_{cb}|$  (points), the result of the fit (solid line) along with its statistical errors (dashed lines), and the function  $\mathcal{F}_{D^*}(w)|V_{cb}|$  obtained from an analysis of  $\bar{B} \rightarrow D^* \ell \bar{\nu}$  decays (dotted line).



TABLE II. Contributions to the systematic error (%) in the fit parameters and partial width. Simulation of the detector and the second  $B$  meson contribute to  $\nu$  simulation.

Source	$ V_{cb} $	$\hat{\rho}_D^2$	$\Gamma$
$\nu$ simulation	11.4	12.5	14.8
Background normalization	7.6	15.4	5.4
$\bar{B} \rightarrow D^* \ell \bar{\nu}$ form factors	1.8	7.1	2.0
$\tau_B$	2.0	2.5	3.8
Lepton ID	1.0	-	2.0
$K/\pi$ ID	0.1	0.7	0.8
Luminosity	0.9	-	1.8
$D$ branching fractions	2.8	-	5.6
Total	14.3	21.2	17.5

TABLE III. Results for various parameterizations of  $\mathcal{F}_D(w)$ . The first errors are statistical and the second are systematic.  $\hat{\rho}_D^2$  and  $\hat{c}_D$  are entirely correlated in the Caprini-Neubert [17] and Boyd [18] models, and fixed in the ISGW2 model [2].

Model	$\mathcal{F}_D(1) V_{cb} /10^{-2}$	$\hat{\rho}_D^2$	$\hat{c}_D$	$\Gamma$ (ns $^{-1}$ )	$\chi^2/\text{dof}$
$\hat{c}_D = 0$	$3.37 \pm 0.44 \pm 0.48$	$0.59 \pm 0.22 \pm 0.12$	0	$12.0 \pm 0.9 \pm 2.1$	11.5/10
$\hat{c}_D$ free	$4.57 \pm 1.10 \pm 0.92$	$1.84 \pm 0.81 \pm 0.53$	$1.75 \pm 1.15 \pm 0.56$	$12.3 \pm 1.0 \pm 2.2$	10.3/9
C-N	$3.90 \pm 0.65 \pm 0.68$	$1.18 \pm 0.37 \pm 0.23$	$0.78 \pm 0.27 \pm 0.17$	$12.1 \pm 1.0 \pm 2.2$	10.8/10
Boyd	$3.71 \pm 0.60 \pm 0.61$	$1.05 \pm 0.38 \pm 0.22$	$0.94 \pm 0.43 \pm 0.25$	$11.9 \pm 0.9 \pm 2.2$	11.1/10
ISGW2	$3.25 \pm 0.13 \pm 0.27$	0.64	0.61	$12.1 \pm 1.0 \pm 2.0$	11.6/11

entire range of  $w$ , we obtain the partial width for the decay. In the fit, shown in Figure 2a,  $\chi^2 = 11.5$  for 10 degrees of freedom, and the correlation between the two parameters is 0.95.

Systematic errors, summarized in Table II, are dominated by uncertainty in the decay model of the non-signal  $B$  and inaccuracies in detector simulation. These effects are investigated by varying the  $K_L^0$  fraction, charm semileptonic decay rate, charged-particle and photon-finding efficiencies, false charged-particle and photon simulation, charged-particle momentum resolution, and photon-energy resolution [15]. Uncertainties in the feeddown background normalizations and the  $\bar{B} \rightarrow D^* \ell \bar{\nu}$  decay form factors [16] have their most significant effect on the form-factor slope. Table III gives results for various models of  $\mathcal{F}_D(w)$ . The partial width is not sensitive to the choice of form-factor parameterization, but the values of  $\mathcal{F}_D(1)|V_{cb}|$ ,  $\hat{\rho}_D^2$ , and  $\hat{c}_D$  are sensitive to this choice. We use these results to determine our model uncertainties.

Our final results are

$$\begin{aligned} \mathcal{F}_D(1)|V_{cb}| &= (3.37 \pm 0.44 \pm 0.48_{-0.12}^{+0.53}) \times 10^{-2} \\ \hat{\rho}_D^2 &= 0.59 \pm 0.22 \pm 0.12_{-0}^{+0.59} \\ \Gamma(\bar{B} \rightarrow D \ell \bar{\nu}) &= (12.0 \pm 0.9 \pm 2.1) \text{ ns}^{-1}, \end{aligned}$$

where the first two errors are statistical and systematic, and the third arises from the form-factor model variations. This partial width leads to branching fractions of

$$\mathcal{B}(\bar{B}^0 \rightarrow D^+ \ell^- \bar{\nu}) = (1.87 \pm 0.15 \pm 0.32)\%$$

$$\mathcal{B}(B^- \rightarrow D^0 \ell^- \bar{\nu}) = (1.94 \pm 0.15 \pm 0.34)\%,$$

where the errors are completely correlated between the two branching fractions. We obtain consistent results when the two decay modes are treated separately. Taking  $\mathcal{F}_D(1) = 0.98 \pm 0.07$  [17], we find  $|V_{cb}| = (3.44 \pm 0.45 \pm 0.49_{-0.12}^{+0.54} \pm 0.25) \times 10^{-2}$ , where the last error arises from the uncertainty in  $\mathcal{F}_D(1)$ . This value of  $|V_{cb}|$  is consistent with those obtained by other means [5,19]. Figure 2b shows the measured values of  $\mathcal{F}_D(w)|V_{cb}|$  and the result of the fit, along with the function  $\mathcal{F}_{D^*}(w)|V_{cb}|$  as measured in  $\bar{B} \rightarrow D^* \ell \bar{\nu}$  decays by CLEO [5]. In comparing these two measurements, we find  $\mathcal{F}_D(1)/\mathcal{F}_{D^*}(1) = 0.96 \pm 0.20$  and  $\hat{\rho}_D^2 - \hat{\rho}_{D^*}^2 = -0.25 \pm 0.29$ . As predicted by HQET, the two form factors have similar normalizations and slopes.

In summary, we have measured the rate normalization and form-factor slope in  $\bar{B} \rightarrow D \ell \bar{\nu}$  decays. The resulting partial width leads to branching fractions for the charged and neutral  $B$  decay modes. The measured form factor parameters are consistent with those measured in  $\bar{B} \rightarrow D^* \ell \bar{\nu}$  decays, as predicted by HQET, and the value of  $|V_{cb}|$  is consistent with other measurements.

We gratefully acknowledge the effort of the CESR staff in providing us with excellent luminosity and running conditions. This work was supported by the National Science Foundation, the U.S. Department of Energy, the Heisenberg Foundation, the Alexander von Humboldt Stiftung, Research Corporation, the Natural Sciences and Engineering Research Council of Canada, and the A.P. Sloan Foundation.

## REFERENCES

- [1] N. Cabibbo, Phys. Rev. Lett. **10**, 531 (1963). M. Kobayashi and T. Maskawa, Prog. Theor. Phys. **49**, 652 (1973).
- [2] N. Isgur and D. Scora, Phys. Rev. D **52**, 2783 (1995). See also N. Isgur *et al.*, Phys. Rev. D **39**, 799 (1989). The form-factor shape is fixed at all orders of  $w$ .
- [3] J.G. Korner and G.A. Schuler, Z. Phys. C **38**, 511 (1988); M. Wirbel, B. Stech, and M. Bauer, Z. Phys. C **29**, 637 (1985);
- [4] N. Isgur and M.B. Wise, Phys. Lett. B **232**, 113 (1989); N. Isgur and M.B. Wise, Phys. Lett. B **237**, 527 (1990); E. Eichten and B. Hill, Phys. Lett. B **234**, 511 (1990); H. Georgi, Phys. Lett. B **240**, 447 (1990); M. Neubert, Phys. Lett. B **264**, 455 (1991); M. Neubert, Phys. Rep. **245**, 259 (1994).
- [5] B. Barish *et al.*, Phys. Rev. D **51**, 1014 (1995); H. Albrecht *et al.*, Z. Phys. C **57**, 533 (1993); D. Buskulic *et al.*, Phys. Lett. B **359**, 236 (1995); D. Buskulic *et al.*, CERN-PPE/96-150; P. Abreu *et al.*, Z. Phys. C **71**, 539, 1996; K. Ackerstaff *et al.*, Phys. Lett. B **395**, 128 (1997).
- [6] Z. Ligeti, Y. Nir, and M. Neubert, Phys. Rev. D **49**, 1302 (1994).
- [7] Y. Kubota *et al.*, Nucl. Instrum. Methods Phys. Res., Sect. A **320**, 66 (1992).
- [8] J. Alexander *et al.*, Phys. Rev. Lett. **77**, 5000 (1996).
- [9] G. Fox and S. Wolfram, Phys. Rev. Lett. **41**, 1581 (1978).
- [10] Particle Data Group, R.M. Barnett *et al.*, Phys. Rev. D **54**, 1 (1996). We use the values  $\mathcal{B}(\bar{B}^0 \rightarrow D^{*+}\ell^-\bar{\nu}) = (4.56 \pm 0.27)\%$ ,  $\mathcal{B}(B^- \rightarrow D^{*0}\ell^-\bar{\nu}) = (5.3 \pm 0.8)\%$ ,  $\mathcal{B}(D^0 \rightarrow K^-\pi^+) = (3.83 \pm 0.12)\%$ ,  $\mathcal{B}(D^+ \rightarrow K^-\pi^+\pi^+) = (9.1 \pm 0.6)\%$ ,  $\tau_{B^-} = (1.62 \pm 0.06)$  ps,  $\tau_{\bar{B}^0} = (1.56 \pm 0.06)$  ps, and  $\tau_{B^-}/\tau_{\bar{B}^0} = (1.03 \pm 0.06)$ .
- [11] J.L. Goity and W. Roberts, Phys. Rev. D **51**, 3459 (1995).
- [12] We assume the following set of decay rates:  $\mathcal{B}(\bar{B} \rightarrow D_1\ell\bar{\nu}) = 0.60\%$ ,  $\mathcal{B}(\bar{B} \rightarrow D_2^*\ell\bar{\nu}) = 0.79\%$ ,  $\mathcal{B}(\bar{B} \rightarrow D_1^*\ell\bar{\nu}) = 0.26\%$ ,  $\mathcal{B}(\bar{B} \rightarrow D_0^*\ell\bar{\nu}) = 0.26\%$ ,  $\mathcal{B}(\bar{B} \rightarrow D'\ell\bar{\nu}) = 0.26\%$ ,  $\mathcal{B}(\bar{B} \rightarrow D^{*'}\ell\bar{\nu}) = 0.53\%$ ,  $\mathcal{B}(\bar{B} \rightarrow (D\pi)\ell\bar{\nu}) = 0.76\%$ , and  $\mathcal{B}(\bar{B} \rightarrow (D^*\pi)\ell\bar{\nu}) = 0.24\%$ , where  $(D\pi)$  and  $(D^*\pi)$  indicates non-resonant production.
- [13] D. Buskulic *et al.*, Z. Phys. C **73**, 601 (1997).
- [14] B. Barish *et al.*, Phys. Rev. Lett. **76**, 1570 (1996).
- [15] K. Bloom, Ph.D. thesis, Cornell University, 1997.
- [16] J.E. Duboscq *et al.*, Phys. Rev. Lett. **76**, 3898 (1996).
- [17] I. Caprini and M. Neubert, Phys. Lett. B **380**, 376 (1996). The form-factor parameterization gives a definite relation between  $\hat{\rho}_D^2$  and  $\hat{c}_D$ .
- [18] C.G. Boyd, B. Grinstein, and R. Lebed, Phys. Lett. B **353**, 306 (1995); C.G. Boyd, B. Grinstein, and R. Lebed, Nucl. Phys. B **461**, 493 (1996); C.G. Boyd and R. Lebed, Nucl. Phys. B **485**, 275 (1997). The form-factor parameterization relates  $\hat{\rho}_D^2$ ,  $\hat{c}_D$  and terms at all orders of  $w$ .
- [19] J.D. Richman and P.R. Burchat, Rev. Mod. Phys. **67**, 893 (1995).